Asian Journal of Chemistry; Vol. 27, No. 11 (2015), 4076-4080

ASIAN JOURNAL OF CHEMISTRY

http://dx.doi.org/10.14233/ajchem.2015.19096

Enhanced Physical and Thermal Performance of Expanded Graphite-Based Heat Sink for LED Radiator

SHU YE, LEI ZHU, ASGHAR ALI, KEFAYAT ULLAH, HAMID ULLAH and WON-CHUN OH*

Department of Advanced Materials Science & Engineering, Hanseo University, Seosan-si, Chungnam 356-706, Republic of Korea

*Corresponding author: Fax: +82 41 6883352; Tel: +82 41 6601337; E-mail: wc_oh@hanseo.ac.kr

Received: 9 February 2015; *Accepted*: 9 March 2015; *Published online*: 16 July 2015; AJC-17406

An experimental study was carried out to investigate the heat transfer characteristics of Cu and Al–modified expanded graphite heat sinks. In this study, the heat sinks were composed of expanded graphite as an active material, Cu and Al as heat transfer enhancement material and resin as a binder. Graphite with high purity was obtained *via* treated with different amount of Na_2CO_3. The as-prepared heat sinks were characterized by XRD, pH, SEM, electrical resistivity, bending strength and thermal analysis. The metal Al modified expanded graphite composite heat sink in our experiment exhibited a good rate of capability in physical and thermal performances. Sample GA5-300 showed highest thermal diffusivity and thermal conductivity.

Keywords: Expanded graphite, Thermal diffusivity and conductivity, Heat transfer.

INTRODUCTION

Expanded graphite (EG) materials as a porous matrix have been inserted into phase change materials due to their high thermal conductivity, chemical stability and bargain price. Being around 90 % volume of expanded graphite connected honeycomb holes, this material has a higher porosity for increasing absorbability and a larger specific surface area than that of graphite. Expanded graphite with these desirable properties attracted researchers paying more attentions in developing high heat performance of thermal energy storage[1-3] and expanded graphite powder has a lower effective thermal conductivity than that of expanded graphite matrix because of its unconnected graphite structure, while has a higher porosity and larger specific surface area. It is more important that the elaboration way of mixing dispersive expanded graphite powder to the molten phase change materials above the melting temperature is much easier than that of cold compression or evacuation infiltration for interconnected graphite matrix. Thus, expanded graphite powder might have a higher potential value than expanded graphite matrix for enhancing heat transfer of phase change materials in real applications[4].

Conventional heat exchangers are mainly constructed from monolithic metals and metal alloys, *e.g.* aluminum and copper. Pure metals including Cu and Al have relatively high thermal conductivities, but their coefficient of thermal expansions of 17 and 23 ppm/K, respectively, are much higher than those of the electronic components which cannot operate at high temperatures[5,6]. These conditions can occur in many thermal management systems[7-9]. As such, metal modified graphite-based plate heat exchangers (PHE) can potentially be considered as an alternative due to their superior performance and thermal characteristics.

Light emitting diode lamps have been assuming a large role in the illumination market, mainly due to their potential in creating not only light but interesting light environments, associated with low power consumption even when compared with other energy saving lamp types[10-12]. Still, from the energetic viewpoint, LED lamps have not yet the desirable efficiency, as a considerable amount of energy is released as heat. This tends to increase the temperature of the LED lamps, leading to a decrease of their lifetime. In order to meet the expected long lifetime, LED lamps must operate below a certain temperature threshold, as given by the manufacturer. To ensure this, the heat sink associated to the LED lamps must provide the needed cooling, requiring the minimum mass of the involved material to obtain the heat sink. Additionally, internal electronic circuitry may have to be activated by cutting the electrical energy to the LED lamp, changing the illumination characteristics, if by any reason some overshoot on the temperature of the LED lamp occurs[13-15].

Heat sinks for LED lamps can operate under natural or forced convection, the first being the preferred ones as neither additional fans nor electric consumption are required. Additionally, noise generation by electric motors and fans is also avoided if natural convection heat sinks are adopted[16].

On the other hand, natural convection heat sinks are thermally less effective, being consequently less compact and heavier and need a careful design to reach the required thermal performance. Heat sinks and LED lamps are assembled together using a thin layer of thermal interface material, which, although designed to have a high thermal conductivity, locally increases the thermal resistance of the assembly[17].

In this work, we report fabrication and interface characterization of oriented Cu and Al–modified expanded graphite heat sink by room-temperature mixing and pressing followed by an optimized pressure infiltration process. The relative density of the composites up to 1.530 g/cm^3 was achieved and graphite flake homogeneous dispersion in composites was obtained. Experimentally obtained effective thermal conductivities and thermal diffusivity of pure expanded natural graphite and expanded natural graphite/metal hydride compacts. Mechanical properties of the composites were also measured.

EXPERIMENTAL

Expansion of graphite: Graphite (KS-6) was selected as the starting material. Expanded graphite was prepared by the method of chemical oxidation. Graphite intercalation compounds (GICs) yielding expanded graphite upon a thermal shock were obtained using chemical oxidation intercalation. 3 g $(NH_4)_2SO_4$ was melted in 100 mL H_2SO_4, then 1 g national graphite was put into the $(NH_4)_2SO_4$-H_2SO_4 solution and stirred at 323 K for 0.5 h. The mixture was carefully washed and filtrated with distilled water until the pH level of the solution reached 7. After being dried at 373 K for 24 h, the graphite intercalation compounds were rapidly expanded at 873 K for 1 h to form expanded graphite.

Preparation of expanded graphite heat sink: The heat sinks were composed of expansion graphite as an active material, Cu and Al as heat transfer enhancement material and resin as a binder. The weight ratio (wt %) of binder was 20 wt %, with a ratio from 0 to 15 wt % was used for metal. Phenolic resin is one kind of thermosetting resin and they are easily poured or formed into any shape, are compatible with most other materials. However, the phenolic resin is brittle and not resistant to high temperature, which often results in wear loss and fade under 350 °C[18]. In order to research the thermal performance of homemade heat sink, calculated amount of phenol resin was added into these different composites and these composites were pressed at a pressure of 80 kg/cm^2, followed by heat treated at two kinds of different temperature as 573 and 673 K for several hours. The heat sinks were prepared with diameter of nomenclatures and prepared method for samples (G-300, G-400, GC5-300, GC5-400, GA5-300, GA5-400) were listed in Table-1. The photographs of the prepared expanded graphite heat sink was shown in Fig. 1.

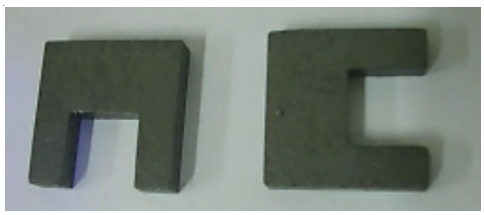

Fig. 1. Photographs of the prepared expanded graphite heat sink

TABLE-1
NOMENCLATURES AND PREPARE METHOD FOR SAMPLES

Sample name	Binder (%)	Metal (%)	Heat treatment (°C)
G-300	20	0	300
G-400	20	0	400
GC5-300	20	Cu 5	300
GC5-400	20	Cu5	400
GA5-300	20	Al 5	300
GA5-400	20	Al 5	400

Characterization and performance of expanded graphite heat sink: XRD (Shimadzu XD-D1, Uki, Kumamoto, Japan) was used to identify the crystallinity of the composite with monochromatic high-intensity CuK_α radiation (λ = 1.5406 Å). Structure of the composite was observed using a scanning electron microscopy (JSM-5600, JEOL Ltd., Tokyo, Japan). pH value was detected by a digital meter (HANNA HI83141, America). In brief, expanded graphite powder (1 g) was dispersed into deionized water with continuous vigorous stirring for 1 h. The suspension was filtered and solution was used to detect the pH value. The electrical resistivity was measured using a Micro ohm meter (SOKEN/DAC-MR-IU, Japan) according to the simplified formula: Electrical resistivity (Ω cm) = {thickness × width × R (mΩ)/length} × 1000[19-21]. Bending strength of different expanded graphite heat sink was also measured. The thermal diffusivity (α, m^2/S) of the different heat sink was measured by a Laser Flash Method (LFA 427, Netzsch). To calculate the thermal conductivity of the samples, the apparent densities (ρ, kg/m^3) of the samples were measured by dividing the mass over the volume and the specific heat capacity (C_p, J/kg K) was measured by diff. scanning calorimetry (DSC 404 C Pegasus). The thermal conductivity (k) is calculated according to the equation: $k = \alpha \times \rho \times C_p$.

RESULTS AND DISCUSSION

Microstructure characterizations: Fig. 2 has shown the XRD pattern of the prepared high-purified graphite. In Fig. 2, the diffraction peak of graphene shifts to higher angle (2θ = 26.2°), respectively. The broad peak at 26.5° corresponding to a d-spacing of 3.35 Å can also be obtained. No impurities can be find from XRD result.

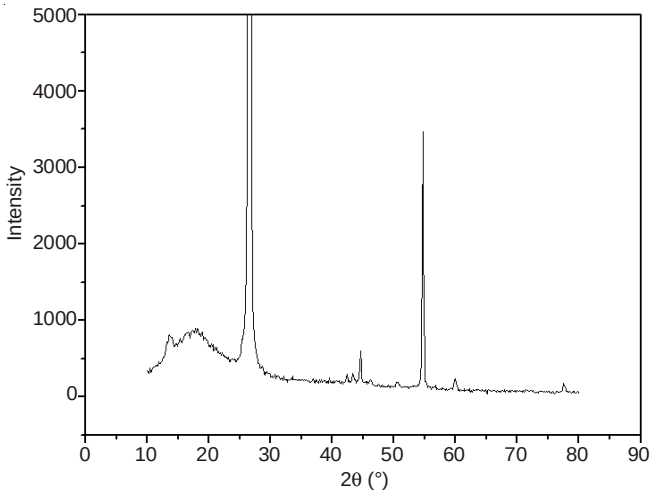

Fig. 2. Typical XRD pattern of high-purified graphite

High purity of prepared samples can also be detected by industrial analysis method such as fixed carbon content (%) = 100 - (Moisture + Volatile Matter + Ash). In order to detect purity of graphite, the mass ratio of graphite to Na_2CO_3 was used as1:1, 1:2, 1:3, followed by heat-treatment at 1023 K or washed with 10 % HCl for 2-3 times and deionized water for 3-5 times. From Fig. 3, it can be observed that the purity was increased to 95.5~99.8 % with increasing the amount of Na_2CO_3. From Fig. 4, it can be observed that the pH value was decreased from 6.98 to 6.96 with increasing the amount of Na_2CO_3. It was indicated that Na_2CO_3 has a great influence on enhancement the purity of graphite and the pH value, thus it can be obtained high-purity graphite with outstanding level of quality.

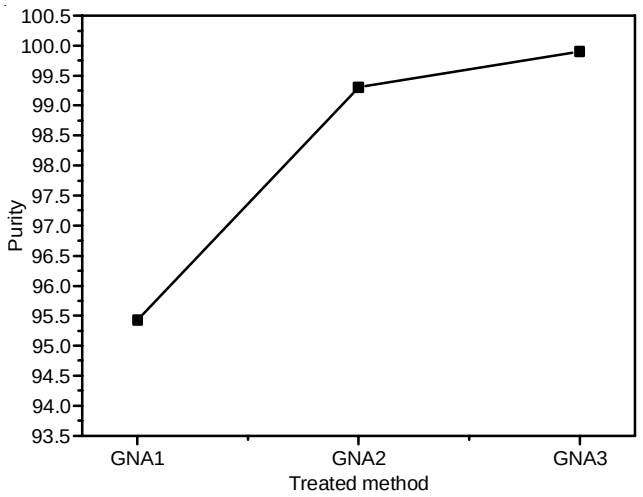

Fig. 3. Purity of high-purified graphite treated by Na_2CO_3 with different amount

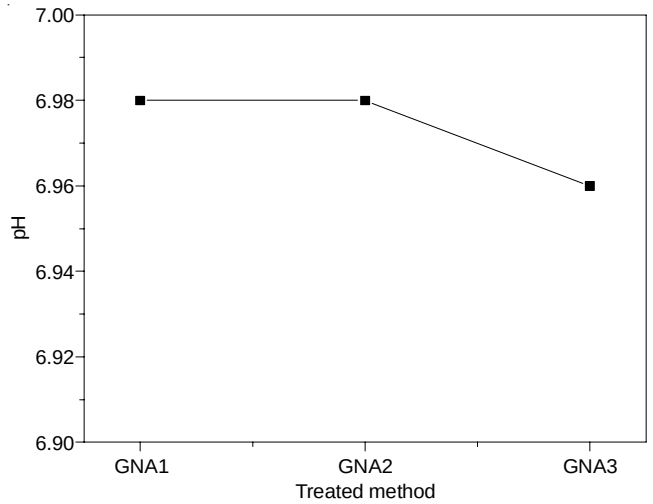

Fig. 4. pH value of high-purified graphite treated by Na_2CO_3 with different amount

The micro-surface structures and morphologies of the treated graphite were characterized by SEM (Fig. 5). The SEM technique is used for inspecting topographies of specimens at very high magnifications, using a piece of equipment called the scanning electron microscope. Fig. 5a and 5b indicates the macroscopic changes in the morphology of graphite before and after purifying. After purifying, small particle size and good smooth surface phenomenon were observed. Thus, we conjecture that graphite has been successfully purified with using appropriate amount of Na_2CO_3. Fig. 5c and 5d show the SEM photomicrographs of expanded graphite. The structure of the layers of graphite flakes was regular and the distance between the layers distance was small. After chemical intercalation treatment and heat treatment at 673~1073 K, it was clearly seen that the spacing of the interlayers of graphite flakes increased and the structure became porous comparing with heat treatment at 473~673 K. This result displays SEM image of a whole graphite nanosheet that appears translucent and owns single crystal graphite structure which agrees with XRD spectra. It demonstrates that the prepared graphite nanosheets are very thin and endowed with the large surface area, which is one excellent property that is responsible for the formation of an electrical conducting within the composite or coating materials at very low graphite contents[22].

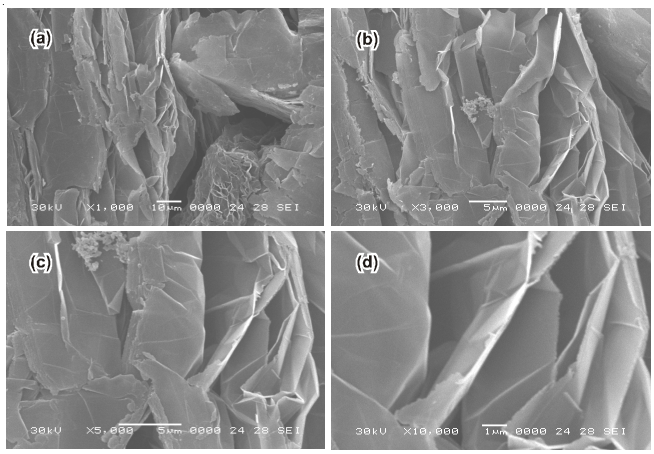

Fig. 5. (a, b) SEM microphotography of graphite before and after purifying, (c, d) SEM microphotography of expanded graphite with different resolution

Physical performances: Fig. 6 shows bending strength is increasing with increasing metal content in metal treated samples (GC5-300, GC5-400, GA5-300, GA5-400) because of the pure expanded graphite is very soft and loose porous material. For pure expanded graphite based sink G-400, the bending strength was higher than that of G-300, it can be speculated that after heat-treatment at higher temperature the sink will become hard due to resin is a binder material. However, after adding metal content the bending strength was changed, it is different with the pure expanded graphite. Due to the metal treated heat sink was composed with metal and expanded graphite, so it could be named as composite materials. Comparing the samples which heat treated at 673 and 573 K, the bending strength was decreasing. It could be speculated that after heat-treatment above 623 K, some amount of resin will be thermally decomposed rapidly thus decrease its viscous force[23]. Fig. 7 showed that the bulk density increases moderately with increasing the metal content. The maximum bulk density is of composite plate with 5 wt % of metal Cu content heat-treated at 573 K. On the other hand, sample GA5-300 also has good result similar than sample GC5-300 which can be speculated that among metal content Al would be an appropriate modification material.

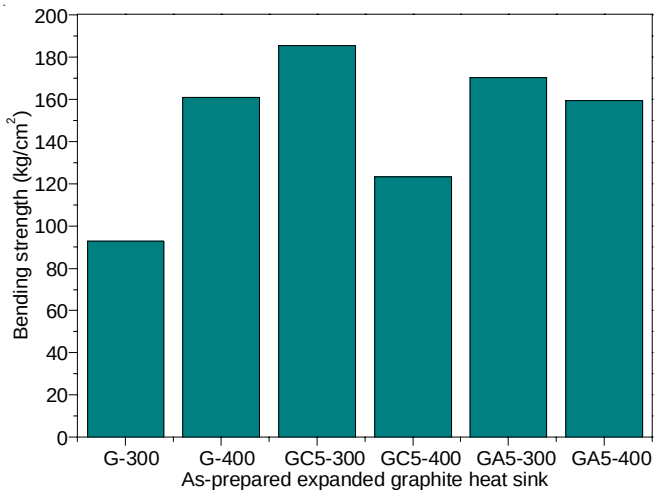

Fig. 6. Bending strength of different expanded graphite heat sink heat treated at 573 and 673 K

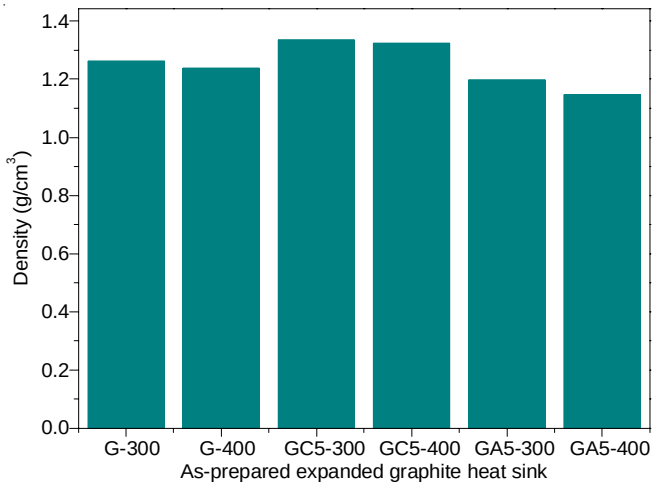

Fig. 7. Density of different expanded graphite heat sink heat treated at 573 and 673 K

The electrical resistivity of the expanded graphite prepared heat sink was measured using a Micro Ohm meter with physical properties analysis method. A diameter and thickness of 1/100 mm, an electric current of 1 A and vertical pressure of 3 MPa were applied on the plate to make a well contact condition between the Ohm meter and specimens. The results of electrical resistivity were shown in Fig. 8. It can be observed that the typical electrical resistivity of the as-prepared samples heat-treatment at 673 K was higher than that of 573 K. Sample GC5-400 has the highest value about 1.42 and GA5-300 has the smaller value about 0.82 comparing with other samples. Meanwhile with adding the different metal, electrical resistivity value was decreased comparing with pure expanded graphite plate.

The thermal diffusivity describes the equilibration of a temperature imbalance. It is a function of thermal conductivity (λ), density (ρ) and specific heat capacity (cp) at a constant pressure. Figs. 9 and 10 show the thermal diffusivity and thermal conductivity of different expanded graphite heat sink heat treated at 573 and 673 K. The thermal diffusivity of pure expanded graphite plate which used as a compared sample is 4.271 and 4.218 mm^2/S heat treated at 573 and 673 K. For pure expanded graphite plate, the thermal diffusivity is almost

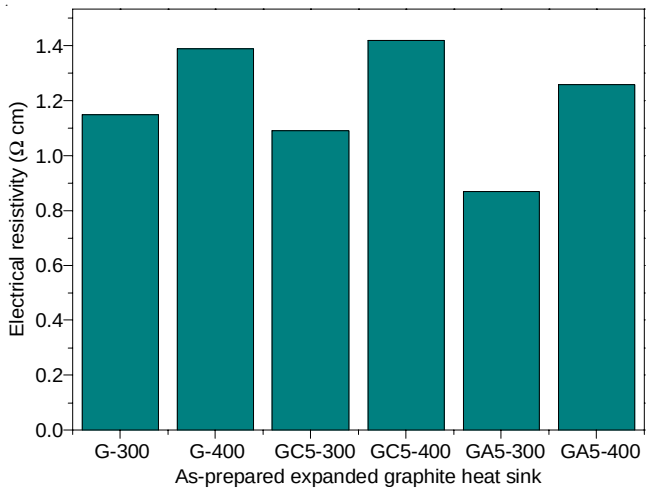

Fig. 8. Electrical resistivity of different expanded graphite heat sink heat treated at 573 and 673 K

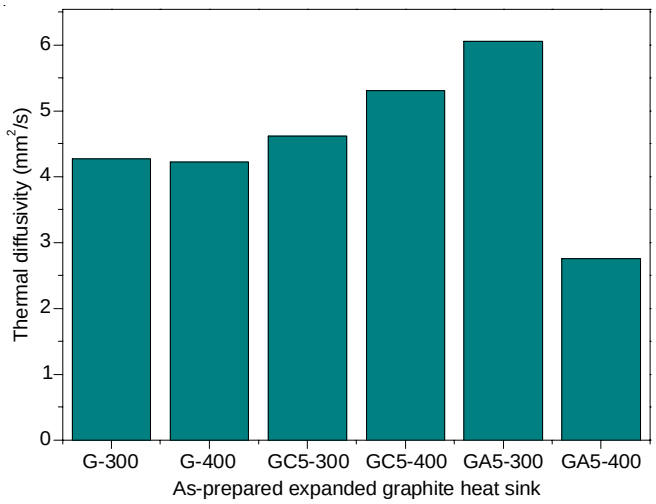

Fig. 9. Thermal diffusivity of different expanded graphite heat sink heat treated at 573 and 673 K

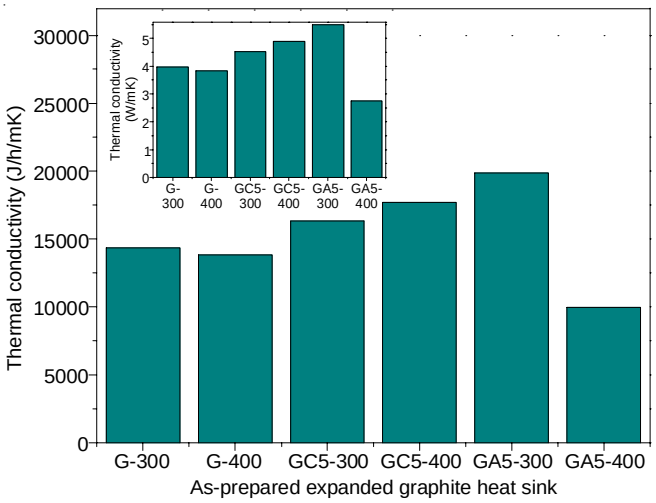

Fig. 10. Thermal conductivity of different expanded graphite heat sink heat treated at 573 and 673 K. (The inset is a thermal conductivity with unit of W/mK)

similar. After metal particles adding to the graphite, the metal-expanded graphite composite plates reveal a significant increase in thermal diffusivity heat treated at 573 K. The thermal

diffusivity of meta-graphite heat sink (GC5-300, GC5-400, GA5-300, GA5-400) is 4.616, 5.303, 6.056 and 2.751 mm^2/S. The thermal diffusivity of metal-graphite composite plates is almost similar with the above results. GA5-300 has the highest thermal diffusivity about 6.056 mm^2/s. It can be considered that the metal particles could enhance the thermal diffusivity of expanded graphite. However, for the samples which treated at 673 K, the results were similar with that of bending strength and density due to the thermal decomposing of resion[23].

From Fig. 10, the thermal conductivity of metal-expanded graphite composite heat treated at 573 and 673 K. Compared with pure expanded graphite sink (G-300, G-400), which has very low thermal conductivity of 14368 and 13827 (J/h)/mK, the metal-expanded graphite composite show a significant increase in thermal conductivity. Among the samples, GA5-300 has the best result as 19856 (J/h)/mK. The inset image is the thermal conductivity with different unit of W/mK about the prepared metal-expanded graphite heat sinks and GA5-300 has the best result as 5.5 W/Mk while the results of G-300, G-400, GC5-300, GC5-400, GA5-400 is 3.98, 3.83, 4.52, 4.9 and 2.75 W/Mk, respectively. Wang *et al.*[24] have studied using compressed expanded natural graphite (CENG) matrices with different densities in an attempt to increase the thermal performance of neopentyl glycol (NPG) for latent heat thermal energy storage (LHTES) application. Measured results indicated that thermal conductivities of the composites can be enhanced 11-88 times as compared with that of the pure neopentyl glycol. According to Chen and Huang[25] current study, it demonstrates that the thermal conductivity and thermal expansion of aluminum-graphite composites can be controlled easily by the percentage of graphite and orientation *via* hot pressing. The process is shown to achieve excellent interface bonding and can avoid detrimental interfacial reactions between aluminum and flake graphite. Based on these published reports, it could be seen that the thermal conductivity of the metal-expanded graphite composite is mainly affected by heated temperature[18] and metal content[6]. These issues could affect the thermal characteristics of composite.

Conclusion

In this study, we investigated the microstructure and physical property metal modified expanded graphite based heat sinks as heat transfer materials. The prepared high-purified graphite was detected by X-ray diffraction. It can be observed that the purity was increased to 95.5~99.8 % with increasing the amount of Na_2CO_3. The structure of the layers of graphite flakes was regular and the distance between the layers distance was small. After chemical intercalation treatment and heat treatment at 673~1073 K, it was clearly seen that the spacing of the interlayers of graphite flakes increased and the structure became porous comparing with heat treatment at 473~673 K. The metal modified expanded graphite composite in this experiment exhibited a good rate of capability in electrochemical performances. GA5-300 showed highest thermal diffusivity and thermal conductivity among these six kinds of expanded graphite composite heat sinks.

ACKNOWLEDGEMENTS

This work was supported by Business for Cooperative R&D between Industry, Academy and Research Institute funded Korea Small and Medium Business Administration in 2013.

REFERENCES

1. T. Ghosh and W.C. Oh, *J. Photocatal. Sci.*, **3**, 17 (2012).
2. M. Sprinkle, M. Ruan, Y. Hu, J. Hankinson, M. Rubio-Roy, B. Zhang, X. Wu, C. Berger and W.A. de Heer, *Nature Nanotechnol.*, **5**, 727 (2010).
3. A. Gao, E. Zoethout, J.M. Sturm, C.J. Lee and F. Bijkerk, *Appl. Surf. Sci.*, **317**, 745 (2014).
4. Z. Li, W.G. Sun, G. Wang and Z.G. Wu, *Sol. Energy Mater. Sol. Cells*, **128**, 447 (2014).
5. A.M. Abyzov, S.V. Kidalov and F.M. Shakhov, *Appl. Therm. Eng.*, **48**, 72 (2012).
6. X.H. Qu, L. Zhang, M. Wu and S.B. Ren, *Prog. Nat. Sci.*, **21**, 189 (2011).
7. L. Zhong, X.W. Zhang, Y. Luan, G. Wang, Y.H. Feng and D.L. Feng, *Sol. Energy*, **107**, 63 (2014).
8. C. Zhou, G. Ji, Z. Chen, M. Wang, A. Addad, D. Schryvers and H. Wang, *Mater. Des.*, **63**, 719 (2014).
9. W.W. Zhao, G. Kido, S. Harada, M. Unno and H. Noguchi, *J. Colloid Interf. Sci.*, **431**, 8 (2014).
10. M. Zamengo, J. Ryu and Y. Kato, *Appl. Therm. Eng.*, **69**, 29 (2014).
11. J.B. Xiao, J. Huang, P.P. Zhu, C.H. Wang and X.X. Li, *Thermochim. Acta*, **587**, 52 (2014).
12. S. Kim, J. Ryu and Y. Kato, *Appl. Therm. Eng.*, **66**, 274 (2014).
13. X.B. Wang, W.F. Zhu, X. Wei, Y.X. Zhang and H.H. Chen, *Mater. Sci. Eng. B*, **185**, 1 (2014).
14. D.X. Li, P.H. Shi, J.B. Wang, J.B. Li and R.J. Su, *Chem. Eng. J.*, **237**, 8 (2014).
15. J.K. Kiplagat, R.Z. Wang, R.G. Oliveira and T.X. Li, *Sol. Energy*, **84**, 1587 (2010).
16. F. Hassouna, A. Laachachi, D. Chapron, Y. El Mouedden, V. Toniazzo and D. Ruch, *Oly. Degrad. Stabil*, **96**, 2040 (2011).
17. C.Y. Zhao and Z.G. Wu, *Sol. Energy Mater. Sol. Cells*, **95**, 636 (2011).
18. U.S. Hong, S.L. Jung, K.H. Cho, M.H. Cho, S.J. Kim and H. Jang, *Wear*, **266**, 739 (2009).
19. P. Krawczyk, *Chem. Eng. J.*, **172**, 1096 (2011).
20. I.M. Afanasov, O.I. Lebedev, B.A. Kolozhvary, A.V. Smirnov and G. Van Tendeloo, *New Carbon Mater.*, **26**, 335 (2011).
21. A. Malas, P. Pal and C.K. Das, *Mater. Des.*, **55**, 664 (2014).
22. Z.D. Meng, K. Ullah, V. Nikam, T. Ghosh, C.Y. Park, H.D. Kwon, S.W. Jang and W.C. Oh, *J. Photocatal. Sci.*, **3**, 113 (2012).
23. Y. Zhang, Y.D. Xu, L.Y. Gao, L.T. Zhang and L.F. Cheng, *Acta Mater. Compos. Sin.*, **23**, 37 (2006).
24. X.L. Wang, Q.G. Guo, Y.J. Zhong, X.H. Wei and L. Liu, *Renew. Energy*, **51**, 241 (2013).
25. J.K. Chen and I.S. Huang, *Composites Part B*, **44**, 698 (2013).